

Characterization of aqueous alcohol solutions in bottles with THz reflection spectroscopy

Peter Uhd Jepsen, Jens Kristian Jensen, and Uffe Møller

DTU Fotonik - Department of Photonics Engineering, Technical University of Denmark,
DK-2800 Kongens Lyngby, Denmark

jepsen@com.dtu.dk

Abstract: We demonstrate a method based on self-referenced THz time-domain spectroscopy for inspection of aqueous liquids, and in particular alcohol solutions, inside closed containers. We demonstrate that it is possible to determine the alcohol content of an aqueous solution, and that liquids can be classified as either harmless or inflammable. The method operates in reflection mode with the result that liquids opaque to THz radiation can be characterized with little influence of the bottle shape. The method works with plastic bottles as well as glass bottles, with absorption of THz radiation by the plastic or the glass being the limiting factor. The reflection mode allows for automatic control of the validity of the measurement. The method will be useful in liquid scanning systems at security checkpoints.

© 2008 Optical Society of America

OCIS codes: (300.6495) Spectroscopy, terahertz; (220.2740) Geometric optical design;
(120.4825) Optical time-domain reflectometry

References and links

1. T. Ikeda, A. Matsushita, M. Tatsuno, Y. Minami, M. Yamaguchi, K. Yamamoto, M. Tani, and M. Hangyo, "Investigation of inflammable liquids by terahertz spectroscopy," *Appl. Phys. Lett.* **87**, 034105 (2005)
 2. N. W. Broad, R. D. Jee, A. C. Moffat, M. J. Eaves, W. C. Mann, and W. Dziki, "Non-invasive determination of ethanol, propylene glycol and water in a multi-component pharmaceutical oral liquid by direct measurement through amber plastic bottles using Fourier transform near-infrared spectroscopy," *The Analyst* **125**, 2054 (2000)
 3. S. Dexheimer (ed.) *Terahertz Spectroscopy: Principles and Applications* (CRC Press, 2007)
 4. P. Uhd Jepsen, U. Møller, and H. Merbold, "Investigation of aqueous alcohol and sugar solutions with reflection terahertz time-domain spectroscopy," *Opt. Express* **15**, 14717 (2007)
 5. P. Uhd Jepsen and B. M. Fischer, "Dynamic range in terahertz time-domain transmission and reflection spectroscopy," *Opt. Lett.* **30**, 29 (2005)
 6. M. Naftaly and R. E. Miles, "Terahertz time-domain spectroscopy of silicate glasses and the relationship to material properties," *J. Appl. Phys.* **102**, 043517 (2007)
 7. H. Kitahara, T. Yagi, K. Mano, M. Wada Takeda, S. Kojima, and S. Nishizawa, "Dielectric characteristics of water solutions of ethanol in the terahertz region," *J. Korean Phys. Soc.* **46**, 82 (2005)
 8. J.-Z. Bao, M. L. Swicord, and C. C. Davis, "Microwave dielectric characterization of binary mixtures of water, methanol, and ethanol," *J. Chem. Phys.* **104**, 4441 (1996)
 9. T. Sato and R. Buchner, "Dielectric relaxation processes in ethanol/water mixtures," *J. Phys. Chem. A* **108**, 5007 (2004)
-

1. Introduction

In the recent years THz radiation, and in particular pulsed, broadband THz radiation, has been applied for demonstrations of imaging with chemical recognition capabilities. The lowest vibra-

tional modes of molecules in their crystalline environment fall in the THz range, so broadband THz spectroscopy is a versatile tool for identification of chemical substances in the crystalline or polycrystalline state. Strongly bound molecular crystals (typically hydrogen-bonded systems such as saccharides) display a strong coupling between phonon modes and molecular vibrational modes. In weakly bound molecular crystals, on the other hand, the vibrational modes are more separated into pure phonon modes and pure molecular modes.

THz radiation penetrates packing materials and clothing. Therefore the use of THz radiation for identification of hidden chemicals has been exploited, at least at the demonstration level. Such potential applications rely on specific spectral features arising from the lowest vibrational modes of the crystal lattice of the chemical substance. Hence the focus have been on inspection of dry, crystalline chemicals.

Liquids have a broadband dielectric response in the far infrared, without sharp and specific spectral features. Polar liquids interact strongly with THz radiation because of the intermolecular hydrogen bonding network. In comparison, nonpolar liquids show a much weaker interaction with THz radiation. While the lack of distinct spectral features hinder specific identification of a liquid, the contrast between polar and nonpolar liquids can be exploited for classification of a liquid. Ikeda *et al.* demonstrated that THz transmission spectroscopy can be used to distinguish between water and inflammable liquids, even through a plastic bottle [1]. Broad *et al.* used near-infrared spectroscopy to determine the distribution of ingredients in multicomponent pharmaceutical liquids, through the wall of amber plastic bottles [2]. Common to these two examples are that although identification is carried out through the plastic bottle wall, the methods rely on a known propagation distance through the liquid, and a transmission measurement.

Here we present an alternative method for the characterization and classification of liquids inside bottles that removes the requirement of a transmission measurement, and at the same time is less sensitive to false negative tests in a scenario where bottles are screened for dangerous (e.g. inflammable or explosive) liquids. We also show that the method can be used to determine the alcohol content of an aqueous liquid inside a bottle.

2. Experimental details

The method is based on the reflection of an ultrashort, broadband THz pulse from the surface of a bottle, as illustrated in Fig. (1). The THz pulse is generated and detected in a standard manner, using photoconductive dipole antennas excited and gated, respectively, by synchronous pulses from a femtosecond laser. The principles of generation and detection of pulsed THz radiation as well as the principles of THz time-domain spectroscopy are described for instance in [3]. As described in detail in a recent publication[4] we make use of the two reflections returned from the bottle, namely the *reference* reflection from the outer surface of the bottle, and the *sample* reflection, returned from the inner surface of the bottle material which is in contact with the liquid. Fig. (1) shows some of the complications that might arise when performing measurements on real bottle shapes. A good identification system should be insensitive to whether the measurement is carried out on the bare bottle, through the label, at the edge of a label, or even through a detached piece of label.

The thickness of the bottle material as well as the topology of the bottle surface will influence the measurement. The thickness of the bottle material determines the temporal separation of the reflected reference and sample pulses, whereas the local topology strongly influences the temporal shape of both the returned pulses.

3. Characterization of bottle materials

Most commercial plastic bottles are made of poly(ethylene terephthalate), or PET. In Fig. (2) we show the optical properties (absorption coefficient and index of refraction) in the THz range

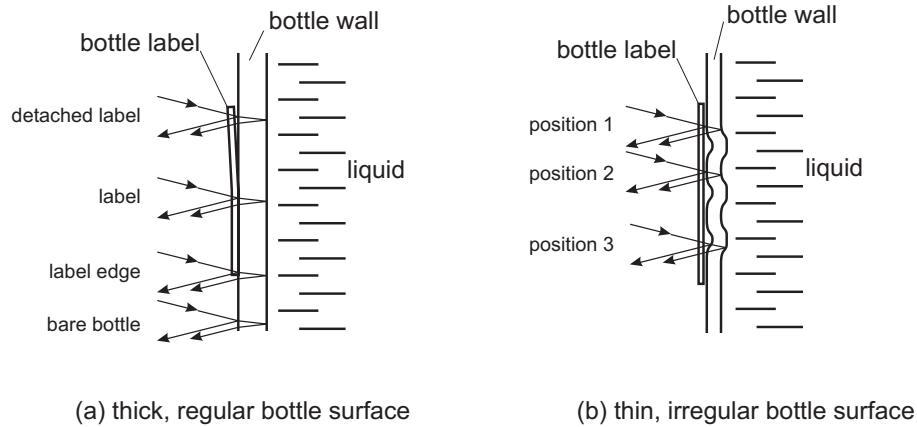


Fig. 1. Definitions of the geometry associated with reflection of the THz signal from a bottle. (a) A thick, regular bottle shape with a paper label and (b) a thin, irregular bottle shape with a loosely attached polymer label.

of different types of PET, compared to those of PMMA, or plexiglass.

The measurements were performed with a standard transmission THz-TDS system. We recorded the optical properties of two commercial polymers Axpet® and Vivak® as well as material cut out from a standard softdrink bottle from one of the major international brands. The absorption spectra of the different PET varieties are similar, and increase monotonically with frequency within our measurement bandwidth. The refractive indices of the PET varieties are similar, to within 0.1.

In Fig. (2) we also show the optical properties of glass cut out from a typical glass bottle. The absorption and index of refraction are shown up to 0.75 THz. Above this frequency the measurement was limited by the available dynamic range of the spectrometer [5].

The absorption coefficient of the glass used in our experiments is higher than the absorption of PET, and the index of refraction of the glass is also higher than that of PET. We note that the optical properties of PET is not too different from those of commercial glasses recently studied by Naftaly and Miles [6]. A more significant difference between PET and glass bottles is the larger wall thickness that in general is required to ensure the mechanical strength of glass bottles, compared to PET bottles. A typical PET bottle for carbonated softdrinks has a wall thickness of 0.65 mm, whereas the wall thickness of a glass bottle with the same volume is 3-4 mm. This, together with the somewhat higher absorption of glass compared to PET, leads to approximately an order of magnitude smaller transmission through a glass bottle wall compared to that of a PET bottle wall.

4. Inspection of liquids inside labeled bottles

We will now investigate the possibility of inspection of the properties of a liquid through the wall of a bottle, possibly covered by paper or plastic labels. For this purpose we filled a PET bottle (0.65 mm wall thickness) with water, and recorded the reflected THz signal from the bottle, with the THz beam incident at various locations on the bottle surface, as illustrated in Fig. (1). Later the measurements were repeated with isopropanol in the bottle. Isopropanol is a flammable liquid with a slightly lower index of refraction and slightly lower absorption coefficient than ethanol. Hence the data shown in this section may indicate how a low-index, volatile liquid can be distinguished from a high-index, non-volatile liquid.

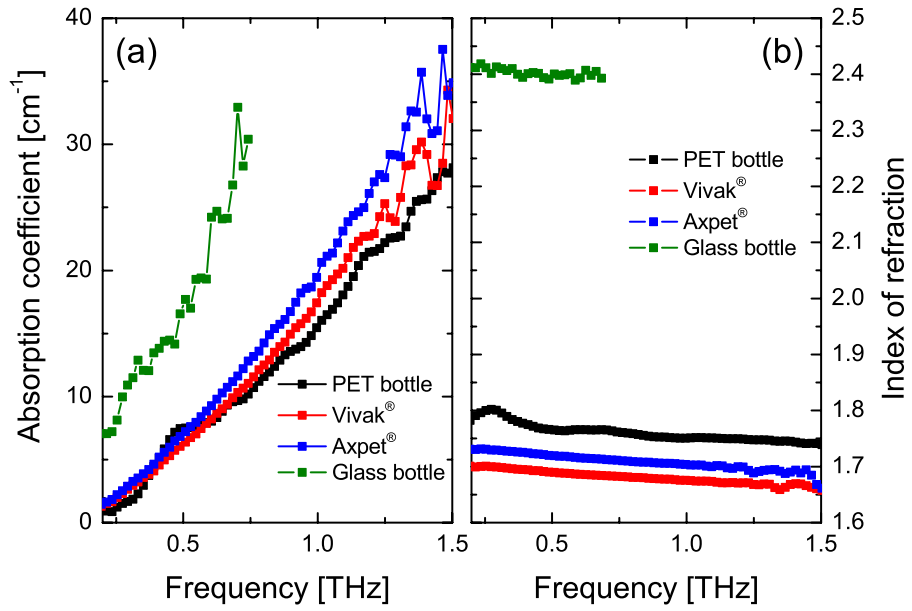


Fig. 2. (a) THz absorption coefficient and (b) index of refraction of PET, in the form of a softdrink bottle (black curves), Vivak®(red curves) and Axpel®(blue curves). The absorption and index of the glass bottle used in this study (dark olive curves) are also shown. All measurements are carried out at room temperature.

Figure 3(a) shows the THz signal reflected from a bare part of the bottle (blue, lower trace), from a position on the bottle completely covered by a paper label (red, middle trace), and from a position on the bottle partly covered by a paper label (green, upper trace). In Fig. 3(b) the reflected signals from similar positions on the same bottle filled with isopropanol are shown. In this plot an additional trace is shown, recorded at a position on the bottle where the label was detached from the bottle.

In all the situations considered in Fig. 3(a) the reflected signal consists of a reference signal and a sample signal, well separated from each other and with a relatively constant temporal shape. Even when the signal is reflected at a point near the edge of the label the signal shape is intact. The additional optical path through the label can be observed as a slight additional delay of the sample signal with respect to the reference signal, compared to the reflected signal from the bare bottle.

The set of measurements on the isopropanol-filled bottle, shown in Fig. 3(b) again show a clear separation between the reference signal and the sample signal. As expected the sample signal is significantly lower than that in Fig. 3(a). In addition the reference signal is strongly modified when the THz beam samples a position on the bottle with a detached label. Here the reference signal splits up due to the additional dielectric interfaces in the beam path. A similar, although less pronounced splitting is observed when we sample at the edge of the label. The reference signal recorded from the edge of the label is different from the similar measurement shown in Fig. 3(a). We took no special precautions to reflect off the exact same location of the bottle in these two situations, so the difference in the reference signal is representative of the spread in signal shapes that might be encountered in the general case.

The influence of atmospheric absorption is seen clearly as additional oscillations in all traces shown in Fig. (3). The experiments were carried out outside of the purged chamber of the THz-

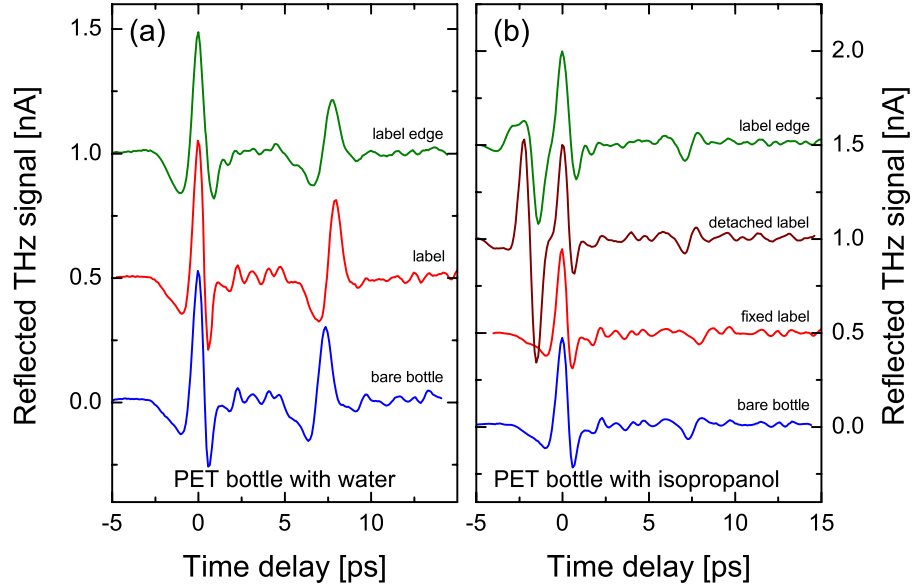


Fig. 3. Reflected THz signals from a PET bottle containing (a) water and (b) isopropanol. The different traces show the reflected signal from a position on the bare bottle, from a position at the edge of the paper label, and from a position on the label.

TDS system, with a THz beam path of 80 cm. Especially when investigating low-index liquids inside the PET container it is seen that the additional oscillations caused by the atmospheric absorption to some extent masks the sample reflection, hence making quantitative measurements difficult. This problem can, however, be minimized by reducing the THz beam path to an absolute minimum, for instance by integrating the THz emitter and detector in a handheld unit that can be brought into contact or to close proximity of the bottle.

Measurements on thinner PET bottles will lead to a smaller separation of the reference and sample signals, as shown in Fig. (4). Here measurements are carried out on a 0.17-mm PET bottle, typically used for still drinking water.

The two lower traces, shown in blue color, show reflected signals from a bottle containing water, and sampled at two different positions on the bottle surface, through the thin plastic label of the bottle. The two top traces, shown in red color, are similar traces recorded at two different positions on the same bottle filled with isopropanol. The variation among the reference signals in the four traces is significant, and the small temporal separation between the reference and sample signal makes a clear distinction between the two signals difficult. However, in spite of the more complicated signal structure compared to reflections from a thicker bottle, the signature of the water is still strong, and easy to distinguish from the isopropanol traces.

5. Simulation of reflected THz signals from bottles

In this section we will present a numerical simulation of the properties of the reflected THz signal from a bottle containing an aqueous solution of ethanol, and show how the reflected signal can be used to predict the alcohol content of the solution.

The reflected THz pulse sequence from the bottle wall can be described in terms of the Fresnel reflection and transmission coefficients of the interfaces of the bottle material. These coefficients are determined by the incidence angle and the optical properties of the bottle mate-

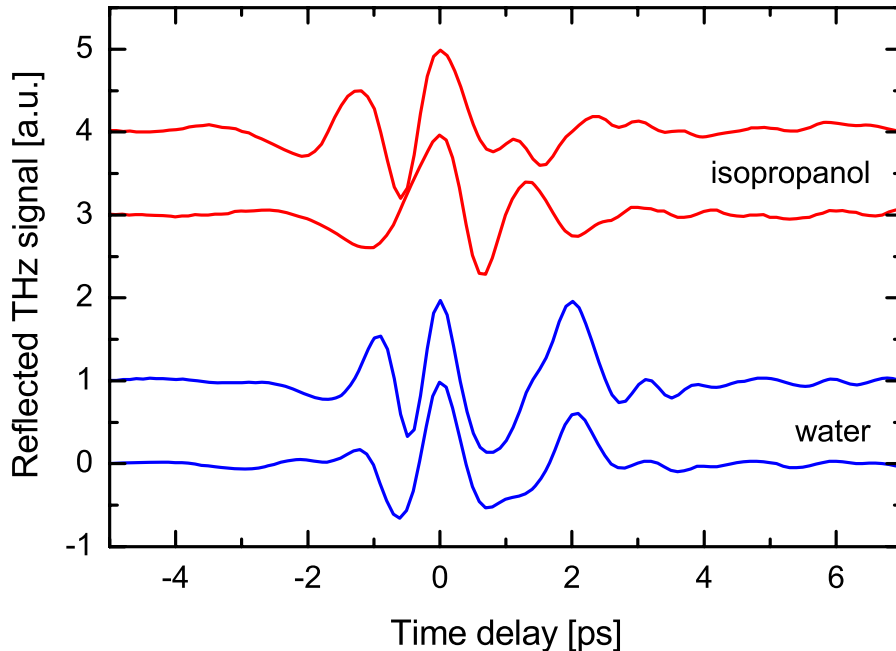


Fig. 4. Reflected THz signals from a thin (0.17 mm wall thickness) PET bottle containing water (lower two traces, shown in blue color) and the same bottle containing isopropanol (upper two traces, shown in red color). Each trace was recorded at a new position on the bottle.

rial and the liquid in the bottle. The reflected field at the angular frequency $\omega = 2\pi v$ from the outer surface $E_{ref}(\omega)$ and the reflected field from the inner surface in contact with the liquid, $E_{sam}(\omega)$, are given by

$$E_{ref}(\omega) = \hat{r}_{12} E_{in}(\omega) \quad (1)$$

$$E_{sam}(\omega) = \hat{t}_{12} \hat{r}_{21} \hat{r}_{23} \exp(-\alpha_2 d_{eff} + 2i n_2 \omega d_{eff}/c) . \quad (2)$$

Here α_2 and n_2 are the absorption coefficient and index of refraction of the bottle material, respectively. The effective path length through the bottle wall, d_{eff} , is defined by the material thickness and the incidence angle. The complex index of refraction of the bottle material is defined in the usual manner, $\hat{n}_2 = n_2 + i\alpha_2 c/2\omega$. For simplicity we will assume that the incident field is TM-polarized.

The reflection and transmission coefficients can be expressed in terms of the external incidence angle ϕ as

$$\hat{r}_{12} = \frac{-\hat{n}_2^2 \cos \phi + \sqrt{\hat{n}_2^2 - \sin^2 \phi}}{\hat{n}_2^2 \cos \phi + \sqrt{\hat{n}_2^2 - \sin^2 \phi}} , \quad (3)$$

$$\hat{t}_{12} = \frac{2 \cos \phi}{\hat{n}_2 \cos \phi + \sqrt{1 - \sin^2 \phi / \hat{n}_2^2}} , \quad (4)$$

$$\hat{t}_{21} = \frac{2\hat{n}_2\sqrt{1 - \sin^2 \phi / \hat{n}_2^2}}{\hat{n}_2 \cos \phi + \sqrt{1 - \sin^2 \phi / \hat{n}_2^2}}, \quad (5)$$

$$\hat{r}_{23} = \frac{-\hat{n}_3^2\sqrt{\hat{n}_2^2 - \sin^2 \phi} + \hat{n}_2^2\sqrt{\hat{n}_3^2 - \sin^2 \phi}}{\hat{n}_3^2\sqrt{\hat{n}_2^2 - \sin^2 \phi} + \hat{n}_2^2\sqrt{\hat{n}_3^2 - \sin^2 \phi}}. \quad (6)$$

The optical properties of the alcohol-water mixture can be described in terms of the Debye model. The Debye model describes the low-frequency and far-infrared dielectric properties of polar liquids within the framework of one or more relaxation processes, each described by a relaxation time τ_i and a dielectric strength $\Delta\epsilon_i$. The dielectric function of the liquid is then

$$\hat{\epsilon}(\omega) = \epsilon_{\infty} + \sum \frac{\Delta\epsilon_i}{1 - i\omega\tau_i} \quad (7)$$

In the literature it has been common to apply two relaxation times (the double Debye model) for the description of the dielectric properties of water, whereas three relaxation processes (the triple Debye model) seem to be required to reproduce the dielectric properties of alcohol. Kitahara *et al.* [7] measured the dielectric function of alcohol/water mixtures, using transmission THz time-domain spectroscopy. They used the triple Debye model to fit all their data in the frequency range 0.1-1 THz. We recently published similar data, obtained by reflection THz time-domain spectroscopy [4], covering approximately the same frequency range. The low-frequency part of the dielectric relaxation spectrum of water-alcohol mixtures is difficult to characterize with THz-TDS. Bao *et al.* published an analysis of the dielectric relaxation spectrum of water/ethanol mixtures in the range 45 MHz - 26 GHz [8], and Sato and Buchner recently published a comprehensive study in the range up to 89 GHz of water/alcohol mixtures[9]. In spite of the available data in the literature there is no consensus on the fitting parameters describing the dielectric function of water-alcohol mixtures. The low-frequency studies by Sato and Buchner [9] seem to overestimate ϵ_{∞} and overestimate the fastest relaxation time τ_3 , due to the lack of data at high frequencies, but that study and also the study by Bao *et al.* [8] firmly characterize the slowest relaxation process. The fitting procedure used by Kitahara *et al.* results in unphysically low values of ϵ_{∞} and extremely fast relaxation processes, of the order of 30-50 fs.

Hence the parameters that give a good agreement between the triple Debye model and the experimental data are not the same in the < 0.1 THz region and in the 0.1-1 THz region. Therefore a goal for future THz research is the recording of the full dielectric function of water-ethanol mixtures at higher frequencies, up to 10 THz.

In spite of these fundamental difficulties with the interpretation of the dielectric function of water-ethanol mixtures we can nevertheless use the triple Debye model to set up a parameterized, phenomenological model for the dielectric function of the mixture for all mass fractions x_{EtOH} of ethanol. We have interpolated the fitted values for the parameters reported by Kitahara *et al.* and slightly modified the values of ϵ_{∞} and $\Delta\epsilon_2$ to reproduce the dielectric function of the neat liquids as recorded by reflection THz-TDS [4].

$$\begin{aligned}\Delta\epsilon_1(x_{EtOH}) &= 69.01 - 48.41x_{EtOH} \\ \Delta\epsilon_2(x_{EtOH}) &= 2.01 - 0.62x_{EtOH} \\ \Delta\epsilon_3(x_{EtOH}) &= 2.08 - 0.87x_{EtOH} \\ \epsilon_{\infty}(x_{EtOH}) &= 2.10 - 0.76x_{EtOH} \\ \tau_1(x_{EtOH}) &= 9.02 + 68.78x_{EtOH}\end{aligned}$$

$$\begin{aligned}\tau_2(x_{EtOH}) &= 0.80 + 0.73x_{EtOH} \\ \tau_3(x_{EtOH}) &= 0.05 + 0.03x_{EtOH}\end{aligned}\quad (8)$$

This parameterization is a simple linear interpolation between the parameter values for neat water and the parameter values for neat ethanol.

In Fig. (5) the real and imaginary parts of the calculated dielectric function of water-ethanol mixtures are shown with solid lines, as function of frequency and ethanol mass fraction. Also shown are the measured real and imaginary parts of the dielectric function of neat water and of neat ethanol.

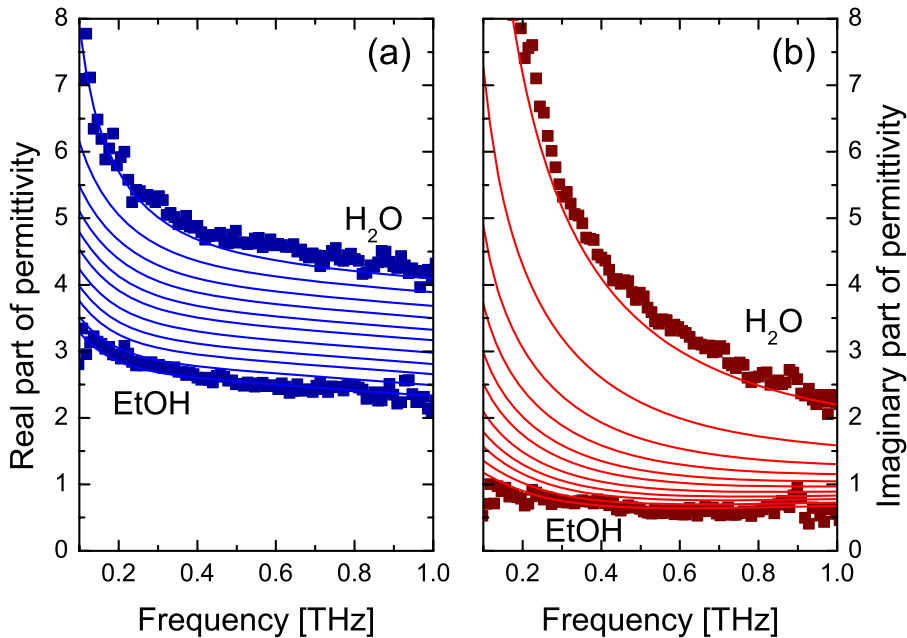


Fig. 5. (solid lines) (a) Real and (b) imaginary part of the modeled dielectric function of water-ethanol mixtures, in 10% increments. The experimental data for neat water and neat ethanol were recorded by reflection THz-TDS. Experimental data for water and ethanol is shown with solid squares.

In the following simulations we will use the triple Debye model with the parameters defined by Eqs. (8) to describe the dielectric properties of water-ethanol mixtures.

6. Inspection of alcohol strength through a bottle wall

We recently used a self-referenced reflection THz spectroscopy technique to determine the alcohol concentration of unknown mixtures of water and ethanol, by placing the liquid on a plane silicon window [4]. Here we use the same self-referencing principle to investigate the optical properties of a liquid, without removing the liquid from its bottle.

In Fig. 6(a) we show the result of a simulation of the return signal from a 0.65-mm PET bottle containing different water-ethanol mixtures. As input pulse for the simulation we used the signal measured in our reflection spectrometer with the PET bottle replaced by a plane, metallic mirror. We applied Eqs. (1) and (2), using the reflection- and transmission coefficients defined in Eqs. (3) - (6) which are calculated using the optical properties of PET and the water-ethanol mixtures discussed above.

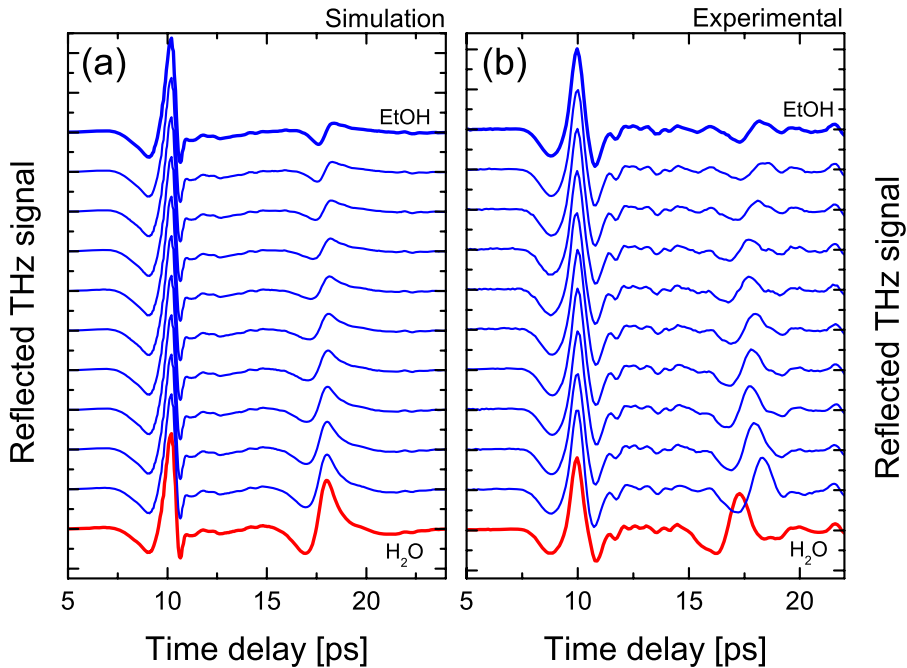


Fig. 6. (a) Simulated and (b) measured reflected THz signal from a PET bottle with 0.65 mm wall thickness, containing mixtures of water and ethanol. The red, lower traces represent the reflection from neat water and each successive curve represents a 10% increase in ethanol mass fraction.

The simulation results show that we should expect a strong sample reflection from a PET bottle containing neat water, and that this reflection should diminish in amplitude with increasing alcohol concentration. Additionally we observe a significant reshaping of the shape of the sample signal. The dispersion of the water-ethanol mixture changes with composition of the mixture. For the highest alcohol concentrations there will be a frequency within our bandwidth with perfect index match between the PET and the liquid mixture. Hence this reshaping is expected.

Figure 6(b) shows the experimental results, obtained under the same conditions as used in the simulation shown in Fig. 6(a), i.e. with a PET bottle of 0.65-mm wall thickness. The PET bottle was removed from the spectrometer between each measurement, for replacement of the liquid. The measurements were carried out at approximately the same spot on the bottle, through the paper label glued to the bottle. No special precautions were taken to ensure the exact same measurement conditions for each scan. The effect of small differences between each scan is seen as slight deviations of the temporal position of the sample reflection with respect to the reference signal due to variations of the bottle wall thickness. The experiment reproduces the simulation quite well. We observe a decreasing amplitude of the sample signal with respect to the reference signal with increasing alcohol strength as well as a significant reshaping of the sample signal. The additional oscillations present in the experimental traces in comparison to the simulated traces are due to water vapor in the THz beam path.

The good agreement between simulation and experiment demonstrated in Fig. (6) indicates that the experimental details left out of the simulation, such as the relatively low radius of curvature of the bottle, the paper label, and the irregular surface, do not significantly influence

the result of the measurements. These geometrical factors will influence the reference signal and the sample signal in approximately the same manner, and hence the ratio of the two signals will be stable against changes in the geometry of the experiment.

In Fig. (7) we show the result of a simulation of the reflected signal from a 3.0-mm glass bottle containing different water-ethanol mixtures. The simulation was carried out as described above, using the optical properties of the glass material shown in Fig. (2).

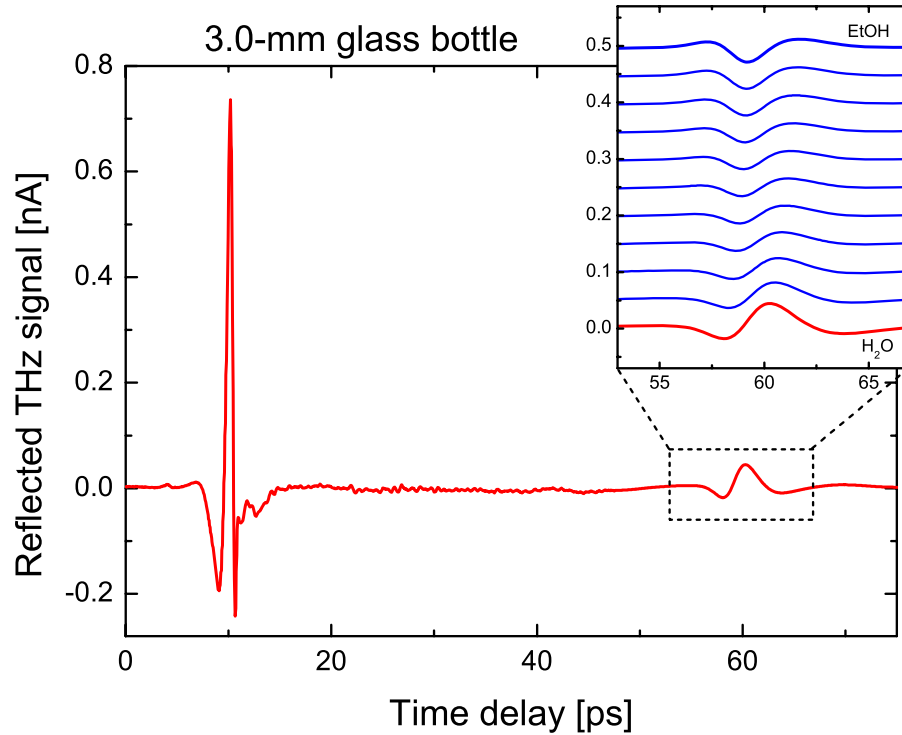


Fig. 7. *Simulated* reflected THz signal from a glass bottle with 3.0 mm wall thickness, containing neat water. The inset shows the shape of the second reflection in dependence of the ethanol concentration in the mixture. The red, lower trace represents the reflection from neat water and each successive curve represents a 10% increase in ethanol mass fraction.

The thicker glass wall compared to the PET bottle, together with the higher index, leads to a delay of 50 ps of the sample signal with respect to the reference signal. The increased wall thickness results in strong attenuation of the sample signal with respect to the reference signal. In contrast to the return signal from the PET bottle, we observe only a modest dependence of the sample signal strength on the alcohol concentration of the liquid. We do, however, observe a significant reshaping of the sample signal that resembles a sign change of the signal, or a 180-degree phase shift. The average refractive index of the glass is located between the refractive indices of neat water and of neat ethanol. Hence, neglecting the frequency dependence of the refractive indices, the sign of the sample signal with respect to the reference signal should change from positive to negative with increasing ethanol concentration. The deviation from the pure sign change is mainly caused by the frequency dependence of the refractive indices of the liquid.

Figure (8) shows the result of a measurement carried out under the same conditions as the

simulation of the reflected signal from the glass bottle.

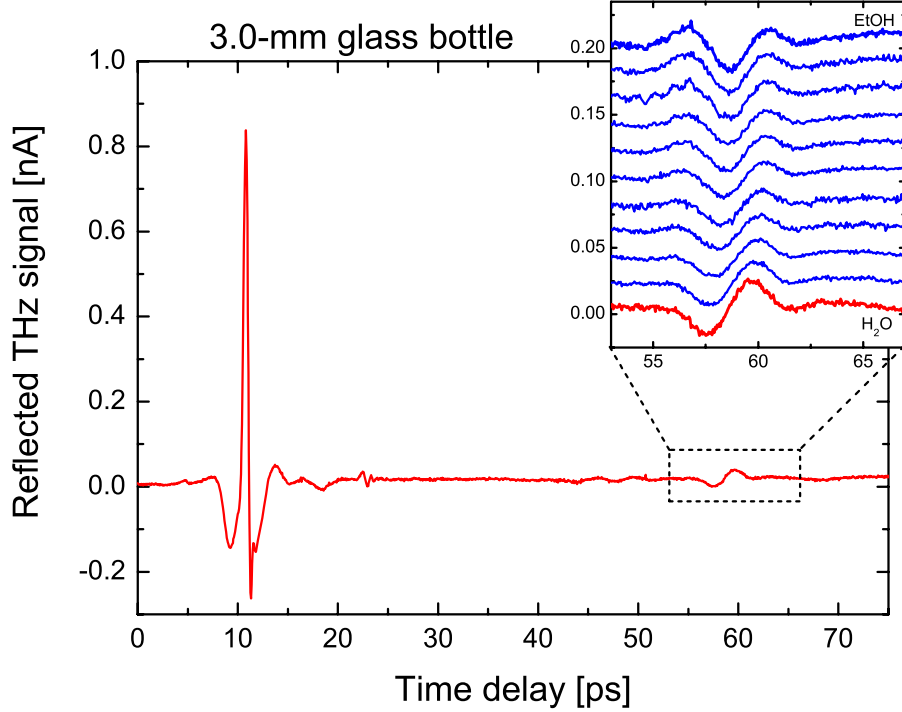


Fig. 8. *Measured* reflected THz signal from a glass bottle with 3.0 mm wall thickness, containing neat water. The inset shows the shape of the second reflection in dependence of the ethanol concentration in the mixture. The red, lower trace represents the reflection from neat water and each successive curve represents a 10% increase in ethanol mass fraction.

There is a good agreement between the simulation results and the experimental data. Experimentally we observe the sample signal 50 ps after the reference signal, and we observe a strong attenuation of the sample signal. The attenuation is slightly stronger than seen in the simulation. We believe that the stronger apparent attenuation could be caused by the displaced reflection plane at the glass-liquid interface with respect to the air-glass interface. The optical path difference between the two reflection planes is 14.4 mm, and the THz beam is incident on the glass bottle at an incidence angle of 30 degrees, focused by an off-axis paraboloidal mirror with an effective focal length of 101.6 mm. Hence the added propagation distance through the glass will lead to some deviation away from the ideal THz propagation axis of the part of the THz signal that is reflected from the glass-liquid interface.

The dependence of the reflected sample signal both from the PET bottle and from the glass bottle on the alcohol concentration suggests that the alcohol concentration x of the liquid inside the bottle can be determined by the ratio of the integrated field strength of the sample pulse and that of the reference pulse. In Fig. (9) we show this ratio R , defined as

$$R(x) = \sqrt{\frac{\sum E_{sam,x}^2(t_i)}{\sum E_{ref,x}^2(t_j)}} \quad (9)$$

where the summation indices i and j are chosen so that the sum covers the full sample- and reference pulses, respectively. The solid, black squares represent the measured ratios, whereas

the solid red curves represent the result of the simulation discussed above. Figure 9(a) shows the results for the PET bottle and Fig. 9(b) shows the results for the glass bottle.

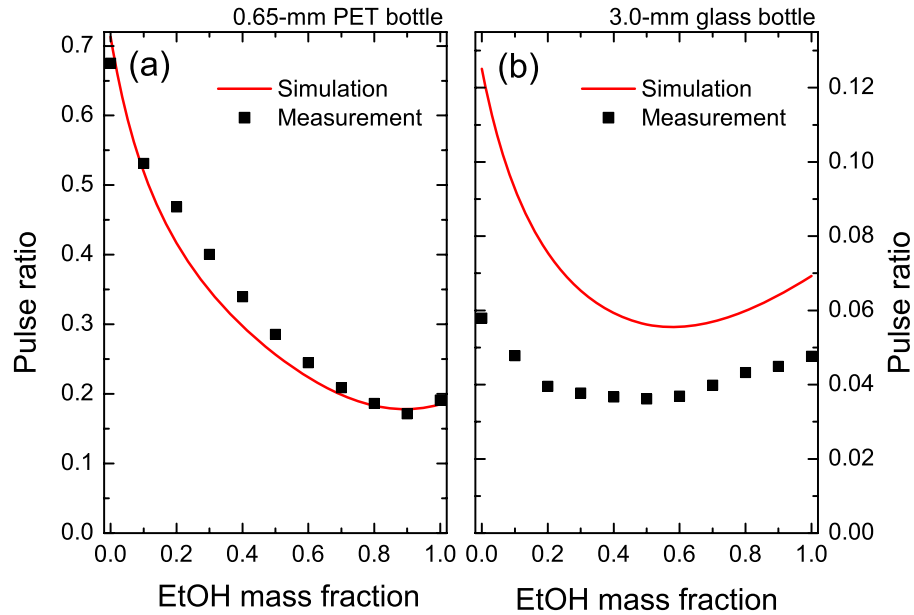


Fig. 9. The ratio of the strengths of the second to the first pulse reflected off an (a) 0.65 mm PET bottle and (b) 3.0 mm glass bottle, as functions of the ethanol concentration of the water-ethanol mixture in the bottles. Red curves represent a simulation, square symbols represent measurements.

The agreement between the experimentally determined ratio and the simulated one is good for the PET bottle, and the monotonous dependence of the ratio on the alcohol concentration allows the determination of unknown alcohol concentrations [4], at least for alcohol concentrations up to 80%. Interestingly both the simulated and measured $R(x)$ increases slightly at the highest alcohol concentrations, indicating that for the highest alcohol concentrations the index of refraction of the liquid crosses that of the PET material. The minimum of the ratio at 90% alcohol concentration corresponds to the best possible index match between the bottle wall and the liquid. The permittivity of PET is 3.06 (see Fig. (2b)). Inspection of Fig. (5) confirms that the highest alcohol concentrations results in a permittivity of the liquid below this value.

For the glass bottle, the measured ratio is lower than the simulated one. The possible reasons for the lower measured ratios are discussed above. The dependence of the ratio on the alcohol content is similar for the simulated and the measured data. The higher refractive index of the glass material shifts the minimum $R(x)$ to lower alcohol concentrations, and results in the observed non-monotonous behavior of $R(x)$. This makes an unambiguous determination of unknown alcohol concentrations in a glass bottle difficult, at least if the ratio R is used as the only estimator.

However, inspection of the progression of the sample signal with alcohol concentration makes it clear that additional information about the composition of the liquid is stored in the significant reshaping of the sample signal. If we for instance use the difference between the sample signal from the bottle filled with the alcohol solution and that from the same bottle with water, $E_{diff,x}(t) = E_{sam,x}(t) - E_{sam,H_2O}(t)$, we can calculate a difference ratio $R_{diff}(x)$ similar

to the ratio defined in Eq. (9) to obtain a signal with a strength that depends monotonously on the alcohol concentration x ,

$$R_{diff}(x) = \sqrt{\frac{\sum E_{diff,x}^2(t_i)}{\sum E_{ref,x}^2(t_j)}} \quad (10)$$

In Fig. 10(a) we plot the sample difference signal $E_{diff,x}(t)$ with varying alcohol concentration x . In contrast to the sample signals themselves, the shape of the difference signals is inde-

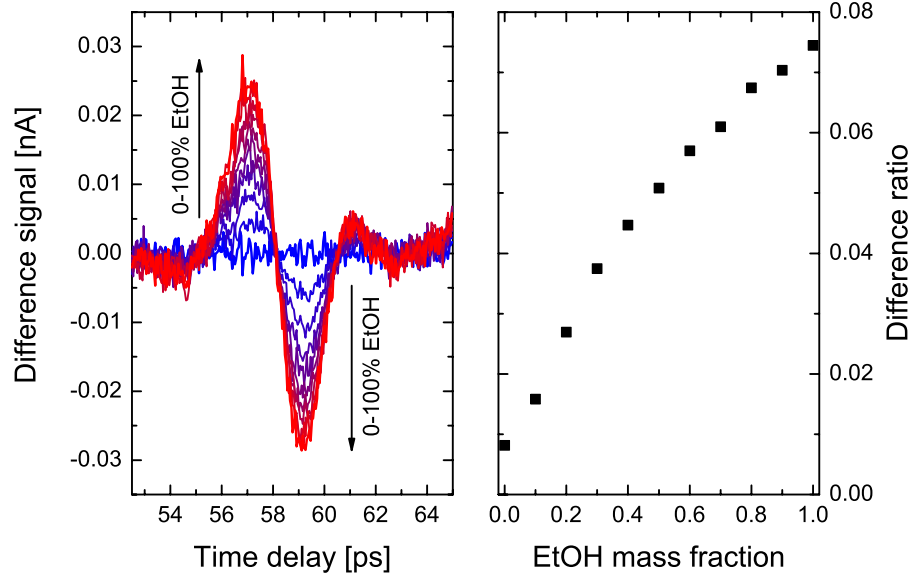


Fig. 10. (a) Time traces of the the difference sample signal reflected from a glass bottle for various ethanol concentrations. (b) The ratio $R_{diff}(x)$ of the strength of the difference signal with respect to the reference signal, as function of alcohol concentration.

pendent of the alcohol concentration, whereas the difference signal strength increases monotonously with alcohol concentration. This indicates that the difference signal is mainly due to the change of the real part of the refractive index of the liquid, and that the additional phase shift associated with changes in the imaginary part of the refractive index has little influence on the reflected signal shape. In Fig. 10(b) the ratio $R_{diff}(x)$ is plotted as function of the alcohol concentration in the bottle. This difference ratio increases monotonously with the alcohol concentration, and is hence useful for the determination of unknown alcohol concentrations in the bottle. The difference ratio shown in Fig. (10) never reaches zero, even for the measurement on neat water. This is due to experimental noise, which is not averaged out in the calculation of the difference ratio since the square of the instantaneous field strength is used in the summations.

7. Conclusions

We have described a method for contact-free inspection of liquids inside bottles. The method relies on the reflection of a THz transient from the bottle. It works by a comparison of the two signals reflected from the bottle; one reflection from the outer surface of the bottle wall and one reflection from the inner surface, in contact with the liquid, of the bottle wall. The automatic generation of a reference signal from the outer bottle surface is useful as a validity check of the

measurement. In contrast to a transmission measurement, where the lack of a transmitted signal in principle can be due to either strong absorption or a misalignment of the system, the lack of any reflected signal clearly indicates an error in the measurement. In a calibrated system the strength of the outer reflection can also be used for automatic identification of the bottle material, based on its index of refraction.

Our experimental and numerical results showed that the method works on both PET bottles and glass bottles. The capability to inspect the content of a glass bottle depends critically on the thickness of the glass, due to the strong absorption of THz waves in the glass material. Hence the dynamic range of the THz detection system is important for the maximum thickness of the glass material. An estimate of the maximal thickness of the glass material is

$$d_{max} \approx \frac{1}{\alpha} \ln(DR) \quad (11)$$

where DR is the dynamic range of the detection system and α is the absorption coefficient of the glass material at the frequency where the dynamic range is defined. For the measurements presented in this work ($DR \approx 1000$ and $\alpha \approx 20 \text{ cm}^{-1}$) we find $d_{max} \approx 0.35 \text{ cm}$.

The concentration of alcohol solutions in PET bottles could be determined by a measurement of the ratio $R(x)$. For the same solutions in glass bottles the simple ratio $R(x)$ is no longer sufficient for an unambiguous determination of the alcohol strength. The difference ratio $R_{diff}(x)$ was introduced to allow determination of unknown alcohol concentrations in a glass bottle. This modified method can then be applied in situations where it is possible to obtain a reflected signal from a similar bottle containing either neat water or neat ethanol.

Acknowledgment

This work was supported by the EU Integrated Project TeraNova.